Transient swelling, spreading, and drug delivery by a dissolved anti-HIV microbicide-bearing film

Cite as: Phys. Fluids **25**, 031901 (2013); https://doi.org/10.1063/1.4793598
Submitted: 01 September 2012 . Accepted: 05 February 2013 . Published Online: 04 March 2013

Savas Tasoglu, Lisa C. Rohan, David F. Katz, and Andrew J. Szeri

PHYSICS OF FLUIDS **25**, 031901 (2013)

Transient swelling, spreading, and drug delivery by a dissolved anti-HIV microbicide-bearing film

Savas Tasoglu,[1,a)] Lisa C. Rohan,[2] David F. Katz,[3] and Andrew J. Szeri[1,b)]
[1]*Department of Mechanical Engineering, University of California, Berkeley, California 94720-1740, USA*
[2]*Magee-Womens Research Institute, University of Pittsburgh, Pittsburgh, Pennsylvania 15213, USA*
[3]*Department of Biomedical Engineering and Department of Obstetrics and Gynecology, Duke University, Box 90281, Durham, North Carolina 22708, USA*

(Received 1 September 2012; accepted 5 February 2013; published online 4 March 2013)

There is a widespread agreement that more effective drug delivery vehicles with more alternatives, as well as better active pharmaceutical ingredients (APIs), must be developed to improve the efficacy of microbicide products. For instance, in tropical regions, films are more appropriate than gels due to better stability of drugs at extremes of moisture and temperature. Here, we apply fundamental fluid mechanical and physicochemical transport theory to help better understand how successful microbicide API delivery depends upon properties of a film and the human reproductive tract environment. Several critical components of successful drug delivery are addressed. Among these are: elastohydrodynamic flow of a dissolved non-Newtonian film; mass transfer due to inhomogeneous dilution of the film by vaginal fluid contacting it along a moving boundary (the locally deforming vaginal epithelial surface); and drug absorption by the epithelium. Local rheological properties of the film are dependent on local volume fraction of the vaginal fluid. We evaluated this experimentally, delineating the way that constitutive parameters of a shear-thinning dissolved film are modified by dilution. To develop the mathematical model, we integrate the Reynolds lubrication equation with a mass conservation equation to model diluting fluid movement across the moving vaginal epithelial surface and into the film. This is a complex physicochemical phenomenon that is not well understood. We explore time- and space-varying boundary flux model based upon osmotic gradients. Results show that the model produces fluxes that are comparable to experimental data. Further experimental characterization of the vaginal wall is required for a more precise set of parameters and a more sophisticated theoretical treatment of epithelium. [http://dx.doi.org/10.1063/1.4793598]

I. INTRODUCTION

An alternative and promising method for blocking sexual transmission of human immunodeficiency virus (HIV) today lies in the application of topical microbicides to mucosal surfaces. There is a widespread agreement that more effective and diverse drug delivery vehicles, as well as better active ingredients, must be developed to increase microbicide efficacy. In this setting, there is now great interest in developing different delivery vehicles such as vaginal rings, gels, and films.

There have been initial fluid mechanical studies of intravaginal fluid flows; these focused on the individual effects of gravity or epithelial squeezing.[1–3] Those initial studies are instructive in developing a physical understanding of the mechanisms of intravaginal vehicle coating flows. The second-generation model developed by our group [4] involves simultaneous effects of a longitudinally

[a)]Present address: Now a post-doctoral researcher at Harvard-MIT Health Sciences and Technology.
[b)]Author to whom correspondence should be addressed. Electronic mail: aszeri@me.berkeley.edu.

directed force along the vaginal canal, e.g., gravity, and transversely directed elastic epithelial squeezing, in a lubrication flow analysis. In follow up, we have analyzed the effects of a yield stress in the elastohydrodynamic flow problem, in the absence of dilution. A yield stress, which constrains gel flow under weak forcing, is emerging as an important property of gel vehicles for microbicide deployment.[5] While it may limit the initial extent of gel coating, it also acts to retain that coating. Thereafter, we supplemented our elastohydrodynamic lubrication model[4] with a convective-diffusive transport equation to model limited amounts of dilution that is inhomogeneously distributed throughout the flowing non-Newtonian fluid.[6] However, this model neglected significant swelling of the gel, owing to restrictions derived from the techniques employed in the analysis. Recently, we have studied the significant swelling of an anti-HIV microbicide gel, and the effects on coating flow.[7]

In many parts of the world, films might be preferred over gels[8] due to their compactness, feasibility of mass production, and better longevity of pharmaceutical components at extremes of moisture and temperature. Therefore films are more appropriate than gels for tropical regions.[9]

In a real application, a microbicide-bearing film dissolves by first imbibing (or taking up) solvent (vaginal fluid), whereupon its material structure changes in a way that frees individual polymer molecules in the film to move. The polymer structural relaxation accompanying water uptake forms a two-phase, glassy-rubbery system, and eventually a single-phase rubbery system. Here, we assume that the relaxation time scale of the polymer network is much smaller than the flow time scale (defined below), and hence we neglect the initial transient dissolution of the film. We develop a mathematical/computational model of the spreading and swelling of a dissolved microbicide-bearing polymer film, and subsequent distribution of an active drug throughout the vaginal lumen. First, the effects of dilution and swelling by ambient vaginal fluids on the rheological properties of the film formulations are experimentally investigated. The rheological parameters are obtained at equilibrium for plausible swelling ratios. We fit a Carreau constitutive model to the rheological data. Then, we integrate the rheological data into a mathematical model of homogeneously diluted film spreading. We explore a plausible mechanism that might drive fluid transport across the epithelial surface boundary, employing a time- and space-varying boundary velocity as a function of osmotic gradient. For the absorption of drug molecules, we employ a transcellular boundary condition. The utility of the present model derives from its ability to afford exploration of physicochemical mechanisms of boundary flux, as well as to treat practical problems such as tradeoffs in film design as they affect the pharmacokinetics.

II. PROBLEM FORMULATION

A. Flow model

In this section, we present a Reynolds lubrication equation[7] which is appropriate to a multi-component mass transfer problem. The equations are developed in the symmetric domain $-h(x, t) \leq y \leq h(x, t)$ and a body force is included in the x-direction. The physical problem and computational domain are sketched in Fig. 1. The model is formulated in a two-dimensional Cartesian domain. The simplification of two-dimensional flow is quite relevant anatomically; the cross section of the undistended human vaginal canal is "H" shaped, with the transverse dimension large compared to the vertical openings on its two sides.[10]

For the constitutive model we take the form

$$\dot{\gamma}_{xy} = \tau_{xy} F(\tau_{xy}). \tag{1}$$

Here, $\dot{\gamma}_{xy}$ is the shear rate and τ_{xy} is the shear stress. One can choose $F(\tau_{xy}) = 1/m_0$ for a Newtonian fluid or, as we do below,[4–6]

$$F(\tau) = \frac{1}{m_0} + \frac{1}{m}\left(\frac{|\tau|}{m}\right)^{(1-n)/n} \tag{2}$$

for a Carreau-like fluid which exhibits shear thinning and a finite viscosity at zero-shear rate, m_0. Here, m is the viscosity of the Carreau-like model and n is the power index. The original

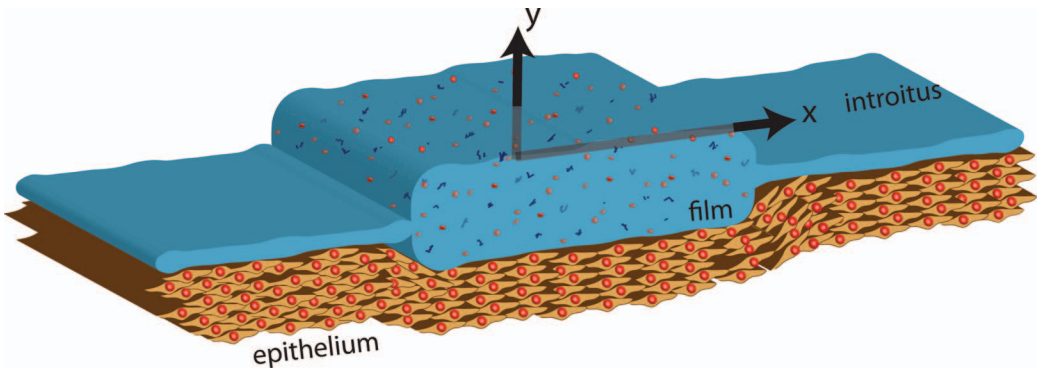

FIG. 1. Definition sketch of the vaginal canal. Epithelium surface is only shown below the film. The introitus is to the right. The transverse direction has an "H" shaped cross section; see text.

Carreau model can be written as $\eta/\eta_0 = (1 + (\lambda\dot{\gamma})^2)^{(n-1)/2}$. Here η is the viscosity of the Carreau model, η_0 is the zero shear viscosity, and λ is the relaxation time of the fluid. The parameters of the Carreau model can be converted into those of Carreau-like model asymptotically[11] in the relationship $m_0 = \eta_0$ and $m = \eta_0/\lambda^{1-n}$. The two models may be matched at small and large strain rates although they are not precisely equivalent.[4]

Following the assumption that we made in Ref. 7, we attempt to simplify our present problem. Similarly, here we assume that the dissolved film-water solution has a homogenous concentration in the transverse direction. This requires the following: $\epsilon^2 \ll 1/Pe$, where the dimensionless P*é*clet number is $Pe = UL/D$, and the representative flow velocity is $U = (MH^3)/(2m_0L)$. Here, $\epsilon = H/L$, and H and L are length scales in transverse and longitudinal directions, respectively. In Ref. 7, after 2 elapsed minutes for typical parameter values, the parameters satisfied the assumption. For films, m_0 is much higher than that of gels, cf. Table I in Ref. 6 and Table I. Therefore, the assumption is well motivated.

With these assumptions, the equations of swelling and spreading of a dissolved film-water solution read as[7]

$$\begin{aligned} \frac{\partial h}{\partial t} + \frac{1}{2}\frac{\partial}{\partial x}\left[\left(M\frac{\partial h}{\partial x} - \rho g\right)m_2\right] &= -q, \\ \frac{\partial(\phi h)}{\partial t} + \frac{1}{2}\frac{\partial}{\partial x}\left[\phi\left(M\frac{\partial h}{\partial x} - \rho g\right)m_2\right] &= \frac{\partial}{\partial x}\left(hD_{fw}\frac{\partial \phi}{\partial x}\right), \\ m_2 &= \int_{-h}^{h}\left[\int_{-h}^{y} F(\tau)y\,dy\right]dy, \end{aligned} \tag{3}$$

where $(1 - \phi)$ is the local volume fraction of the added water, and ϕ is the local volume fraction of the pharmacological vehicle. As in our earlier works, we employ the one-dimensional constrained

TABLE I. The parameters of the Carreau-like model (m_0, n, and m) for a dissolved prototype film. Yield stress of the film dilution samples (1 batch for each dilution).

Swelling ratio	m_0 (Pa s)	n	m (Pa s^n)	Yield stress τ_0(Pa)
3	5843.92	0.3394	222.82	23.81
4	1777.35	0.4960	104.21	2.94
5	671.077	0.6036	70.99	0
8	652.69	0.6628	10.65	0

continuum[11] approximation to model vaginal wall elasticity.[12–14] In this approximation, the fluid pressure near a compliant wall is proportional to the local deformation of that wall. In general, for a deformation h, the fluid pressure is given by $p = (E/T)h \equiv Mh$. Here, E is the elastic (Young's) modulus of the compliant layer, T is its thickness, and M is the compliance of the elastic wall. We take for that compliance the representative value 10^4/0.5 Pa/cm.

The boundary fluid velocity, $q(x, t)$ is a quantity that is not well understood. There is remarkably little research on the quantity and flow of human vaginal fluid.[15,16] This fluid is produced primarily by a transudation process through the vaginal epithelium.[15] In general it is believed that the rate of fluid percolation through the vaginal epithelium may be variable, depending upon the time of day, the phase of the menstrual cycle, and/or other factors. It is also increased during sexual stimulation.[16] In principle, vaginal fluid flow out from the epithelial surface and into a film coating may be affected by osmotic phenomena, and/or by the hydrodynamic pressure in the vaginal lumen. Here, absent more detailed physiological information, we shall explore a potential mechanism and associated boundary condition, wherein the fluid velocity across the epithelial surface boundary is taken as dependent on the osmotic pressure gradient. At the end of the paper we will discuss relevant measurements that need to be performed in order to progress further in this problem.

B. Drug distribution model

In addition, we shall model the subsequent distribution of active ingredient throughout the vaginal lumen. A recently completed study[17] has shown significant effectiveness of the anti-HIV compound Tenofovir in blocking HIV transmission in women. Here, we study a case of Tenofovir-bearing film formulations. Very simply, another mass conservation equation could be added to the multi-component model (Eq. (3)) in order to model drug distribution. However, this would require the assumption of uniform concentration of drug in the y-direction.

To the best of our knowledge, there is no reported value for the diffusion coefficient of Tenofovir molecules in water, D_T. Here, we approximated D_T using experimentally defined diffusion coefficients of a compound of similar molecular weight, fluorescein.[18] The moleculer weights, MW, of fluorescein, dapivirine, and Tenofovir are: 332.3 g/mol, 329.4 g/mol, and 287.2 g/mol, respectively. The experimentally measured diffusion coefficients of water and fluorescein in water are: 2.2×10^{-5} cm^2/s and 4.86×10^{-6} cm^2/s.[18] For convenience, we approximate the diffusion coefficient of Tenofovir molecules in water (and in dissolved film-water solution) as $D_T \approx 10^{-6}$ cm^2/s. On the other hand, the diffusion coefficient of water molecules in water (and in dissolved film-water solution) is taken as $D_{fw} \approx 10^{-5}$ cm^2/s. Here, we shall assume that the transport of Tenofovir molecules in both the x- and y-directions should be taken into consideration, because D_T is one-tenth of that of water in film-water solution, D_{fw}.

Now, we return to the model that we developed in Ref. 6 for 2D water distribution with a moving boundary and for modest dilutions. We employ that model here for the transport of Tenofovir molecules along the vaginal lumen and subsequent absorption of them at the vaginal wall. With the domain mapping $(x, y) \rightarrow (x, \zeta)$, the two-dimensional convection-diffusion equation defined in (x, y) domain[6] with the shape of a film transforms into an equation defined in (x, ζ) domain with the shape of a rectangle. Here, $y = h(x, t)\zeta$. The domain (x, ζ) has the shape of a rectangle instead of the shape of the film and the grid points in the ζ- direction are fixed for every time step. The tranformed equation reads[6]

$$\frac{\partial \Psi}{\partial t} = -u_1 \frac{\partial \Psi}{\partial x} - \frac{1}{h}\frac{\partial \Psi}{\partial \zeta}\left[u_2 - \zeta\left(\frac{\partial h}{\partial t} + u_1 \frac{\partial h}{\partial x}\right)\right] + \frac{D_0 exp(a_d V)}{h^2}$$
$$\times \left\{-\zeta h(1 + a_d V)\frac{\partial^2 h}{\partial x^2}\frac{\partial \Psi}{\partial \zeta} + (2a_d + a_d^2 V)\left(\frac{\partial \Psi}{\partial \zeta}\right)^2 + (1 + a_d V)\frac{\partial^2 V}{\partial \zeta^2}\right.$$
$$\left. + \zeta\left(\frac{\partial h}{\partial x}\right)^2\left[2(1 + a_d V)\frac{\partial \Psi}{\partial \zeta} + (1 + a_d V)\frac{\partial^2 \Psi}{\partial \zeta^2} + a_d \zeta(2 + a_d V)\right.\right.$$

$$\times \left(\frac{\partial \Psi}{\partial \zeta}\right)^2\Bigg] - 2\zeta h \frac{\partial h}{\partial x}\left[a_d(2+a_dV)\frac{\partial \Psi}{\partial \zeta}\frac{\partial \Psi}{\partial x} + (1+a_dV)\frac{\partial^2 V}{\partial \zeta \partial x}\right]$$
$$+ h^2\left[a_d(2+a_dV)\left(\frac{\partial \Psi}{\partial x}\right)^2 + (1+a_dV)\frac{\partial^2 V}{\partial x^2}\right]\Bigg\}, \quad (4)$$

where $h = h(x, t)$, and velocity components in the x- and y- direction are $u_1 = u_1(x, y, t)$ and $u_2 = u_2(x, y, t)$, respectively. Here, Ψ is the concentration of Tenofovir, and $\Psi = \Psi(x, \zeta, t) = \psi(x, y, t)$. The flow equations, Eq. (3) and transport equation for Tenofovir molecules, Eq. (4) are solved together in a multi-step implicit numerical scheme. Here, the assumption that D_T is dependent on the volume fraction of Tenofovir as $D_T = D_0 exp(a_d\Psi)$,[19] enable us to take into consideration further interactions of Tenofovir with the vaginal wall.

III. RESULTS

We shall first experimentally investigate the effects of dilution and swelling by ambient vaginal fluids on the rheological properties of the film formulations designed for vaginal microbicide drug delivery. The extent to which films swell depends on the amount of vaginal fluid absorbed and can be quantified using the parameter called the swelling ratio,

$$\text{Swelling ratio} = \frac{\text{Mass of imbibed fluid}}{\text{Mass of dry film}}. \quad (5)$$

The amount of ambient fluid present in the vaginal canals varies between individuals, ranging from 0.5 g to 0.75 g (assuming the vaginal fluid density of 1 g/cm^3). Current applications of vaginal films apply the materials in a size of approximately 25.8 cm^2. The weight of our film formulation of this size is approximately 0.17 g. Therefore, assuming complete dissolution by only already-available vaginal fluid, the net swelling ratio of films in vaginal fluid in real application can be estimated as ranging from 3 to 5. If other vaginal fluid is recruited via the mechanisms explored later in this paper, the swelling ratio may be larger.

Now we turn to an assessment of the rheology of dissolved film solutions. Film and de-ionized (DI) water were appropriately massed to obtain the desired dilutions. The film was then dissolved in the water in a microtube. The film solutions were homogenized via mixing by vortexing. The diluted solutions were capped and allowed to equilibrate for approximately 24 h before taking measurements. Multiple batches of samples were prepared. For each dilution, results were averaged from 3 independent batches.

The measurements of the rheological properties of the film were obtained on a TA Instruments model AR 1500ex rheometer using a 4° cone and 20 cm diameter plate. Measurements were taken at 37 °C over shear rates in the range of 0.01 − 500 s^{-1} in order to simulate the shear rates in which materials (film and film-like materials) experience in real application. That is, the materials experience shear rates of less than 0.1 s^{-1} during passive seeping and shear rates approximately 100 s^{-1} during coitus.[20] Yield stress measurements were taken from measuring the residual stress at 37 °C with a Brookfield model 5 HB DV-III Ultra rheometer.

A. Experimental results

The log-log plots of viscosity vs. shear rate of films (blue dots) and fitted Carreau model (red lines) are given in Fig. 2 for swelling ratios: 3, 4, 5, and 8 (left to right, top to bottom).

Table I shows that the zero shear viscosity m_0 decreases significantly (to one-tenth) and the shear-thinning exponent n doubles as swelling ratio increases from 3 to 5, i.e., estimated range of swelling ratio in real applications. Yield stress is also obtained by measuring the residual stress of each film dilution sample. Results show that the film begins to lose its yield stress as the degree of dilution increases. For this particular film, it completely loses its yield stress when the swelling ratio becomes greater than 4.

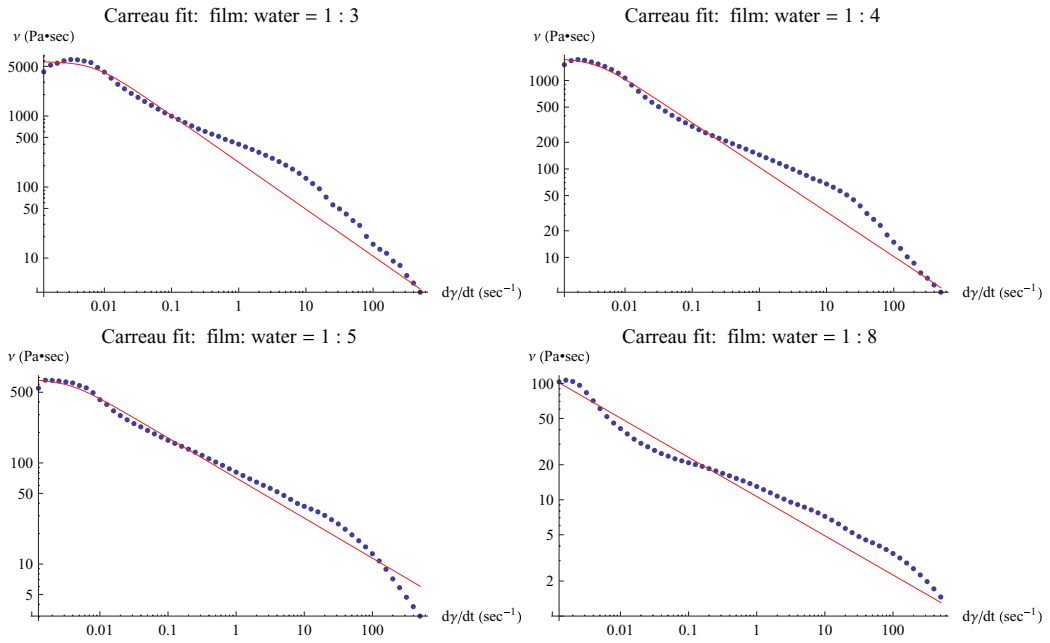

FIG. 2. The log-log plot of viscosity vs. shear rate of a prototype film with swelling ratio: 3, 4, 5, and 8. Dots are experimental data, and the solid (red) line is the fitted Carreau model.

B. Homogeneous spreading

Now, we integrate the rheological data of the film formulations into the mathematical model of the coating flow. Here, the initial condition for the height profile of a film is

$$h(x, t = 0) = \begin{cases} h_\infty & \text{if } x < -a/2 \text{ or } x > a/2 \\ b & \text{otherwise,} \end{cases} \tag{6}$$

where a is the width of the film, b is the initial height of the film ($= vbsr \times h_\infty$). Here, $vbsr$ is a volume-based swelling ratio, calculated by multiplying the original swelling ratio with the density ratio of film and water (ρ_f/ρ_w). To smooth the corners of the film at $x = \pm a/2$, an error function is used in a way that it covers ten grid points (1/40 of the grid points in the x-direction). Although it is not presented here, further increase in the number of grid points did not change the results.

As an initial approach to effects of film dilution on flow, we assume that the mixing ratio of film and vaginal secretions is constant and that dilution is homogeneous during the spreading process. In other words, in this section, *there is no further dilution after the onset of flow*. The film formulations are already swollen, and ready to spread.

Results are illustrated in Fig. 3 for the profile of the film at 2 h after the onset of flow. The height profiles are shown for swelling ratios = 3, 4, 5, and, 8. The spreading length of the film increases with the extent of swelling ratio. In order to quantify the effect of swelling ratio clearly, the coated area is shown in Fig. 3(b). The length of spreading of the film, which is proportional to the effective surface area coated, we define as four standard deviations of the film height profile.[4] Then, this is multiplied with the physical width of the vagina, i.e., 2 cm. The effect is clearly significant; for example, a prototype film with swelling ratio 5, coats in 2 h three times the area compared to a film with swelling ratio 3. On the other hand, film formulations with a range of swelling ratio 3–5, i.e., estimated range in real applications, coat less area than homogeneously diluted gels accomplish. This can be partially attributed to the rheology of the film formulations.

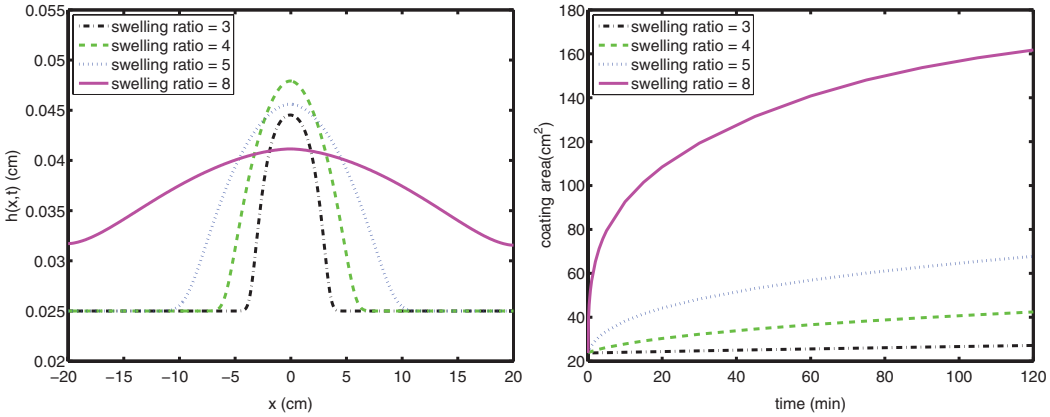

FIG. 3. (Left) Height profile of films at 2 h and (right) coating area of the film on the surface for swelling ratio = 3, 4, 5, and 8.

C. Transient swelling and spreading

A microbicide-bearing polymer film dissolves by first imbibing (or taking up) solvent (vaginal fluid), whereupon its material structure changes in a way that frees individual polymer molecules in the film to move. The polymer structural relaxation via water uptake forms a two-phase, glassy-rubbery system, and eventually one-phase, fully rubbery system. An important question arises here: Does this phenomenon occur under the conditions where the relaxation time scale of polymer molecules is comparable to the flow time scale? We assume that the relaxation time scale of the polymer network is much smaller than the flow time scale, and neglect the transient dissolution of the film. Instead, in this section, we develop a model for additional transient swelling and spreading of a dissolved film deploying anti-HIV microbicide, after the rubbery transition. In our model, we consider further swelling of film, and subsequent distribution of microbicides throughout the vaginal lumen. The association between swelling of film and rheological properties is obtained experimentally, delineating the way constitutive parameters are modified by swelling and dilution. The hyperbolic curve-fits of the results given in Table I are found to be

$$\begin{aligned} m_0 &= 562 - 0.908 \cdot \sinh(-13.93 + 2.54 \cdot vbsr), \\ n &= 0.68 + 0.00084 \cdot \sinh(-8.77 + 1.15 \cdot vbsr), \\ m &= -43.56 + 3.207 \cdot \coth(-0.0146 + 0.0148 \cdot vbsr). \end{aligned} \tag{7}$$

The constitutive parameters, m_0, m, and n of the Carreau-like model are plotted in Fig. 4.

It is known that vaginal fluid is produced primarily as the result of an exudation process across the vaginal epithelium.[15] There is insufficient experimental data at present to enable creation of a definitive fluid transport boundary condition on the surface of the vaginal epithelium. For this reason, we shall now explore a potential mechanism that could be associated with production of vaginal fluid at the epithelial surface. We draw upon knowledge of related boundary conditions on other tissue surfaces.

1. Boundary flux dependent on the osmotic gradient

We first consider a model in which the boundary flux is related to a significant osmotic gradient across the epithelial surface. We assume that vaginal epithelium, at the ultrastructural level, consists of long, narrow paracellular transport channels open at one end (apical/lumen side) and closed at the other (serosal side), see Fig. 5. Solute (NaCl) is actively transported into the lateral intercellular spaces (LIS, lying along the z axis in Fig. 5) across its walls, making the channel fluid hypertonic. As solute diffuses towards the open mouth, more and more water enters the channel along its length due to the associated osmotic gradient. In the steady state a standing osmotic gradient would be maintained in the channel by active solute transport. We closely follow a model developed in

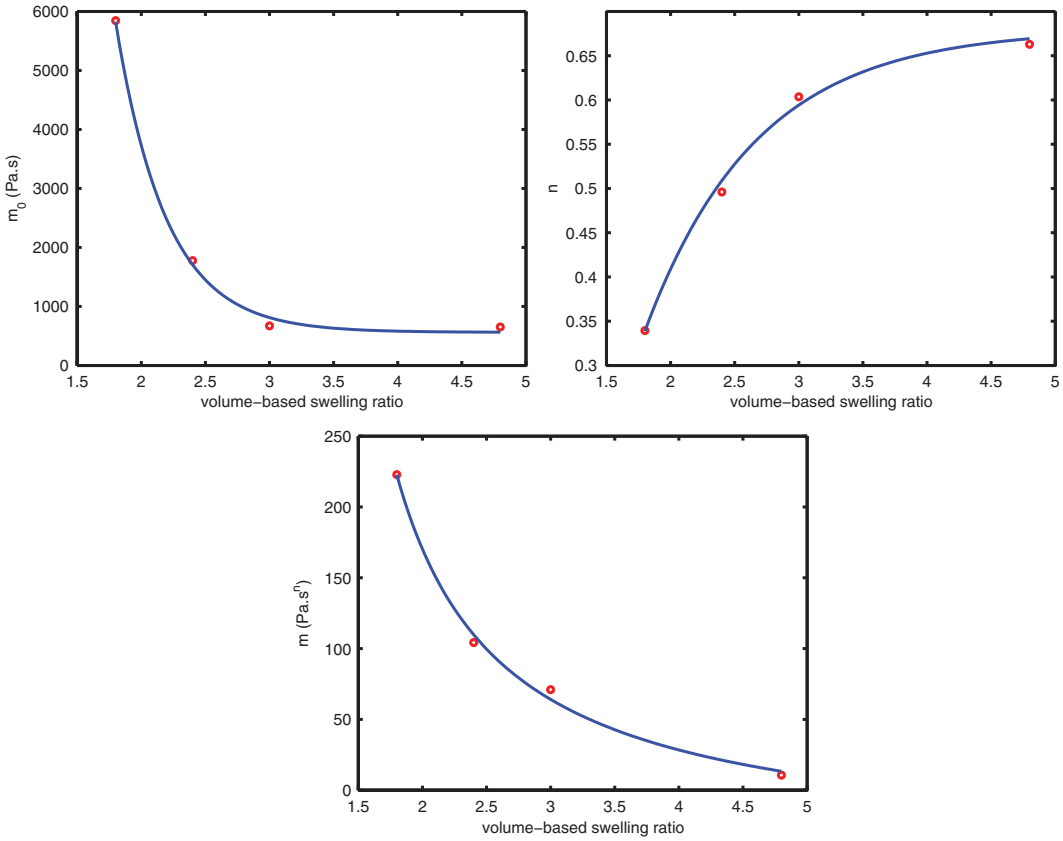

FIG. 4. Curve fit to Carreau-like zero-shear viscosity (m_0), power index (n), and viscosity (m) data of a prototype film. Solid line is hyperbolic curve-fit and dashed line is quadratic curve-fit.

Ref. 21. However, the model is extended here to apply to the case where the external solution (at $z = L$) may have different osmolarity from the cell interiors. With this change, the governing equation for the velocity of fluid in the channel is given as

$$N(z) + \frac{D_s r^2}{4P}\frac{d^3 v}{dz^3} - \frac{r^2}{4P}\nu\frac{d^2 v}{dz^2} - \frac{C_i r}{2}\frac{dv}{dz} - \frac{r^2}{4P}\left(\frac{dv}{dz}\right)^2 = 0. \tag{8}$$

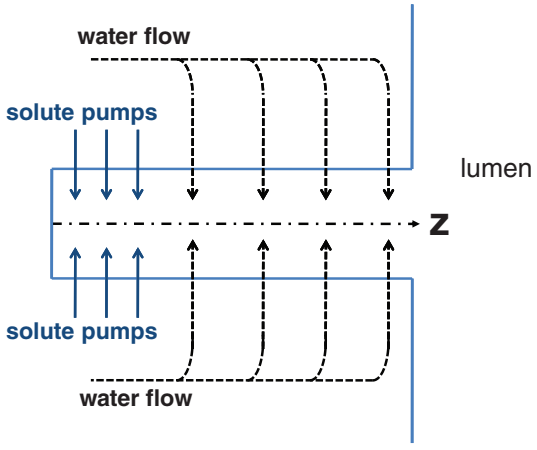

FIG. 5. Sketch of a standing-gradient flow system.

Here, the independent parameters are

- L = the length of the paracellular transport channel,
- r = the radius of the channel,
- P = the osmotic water permeability of the channel walls, defined as the volume of water crossing 1 cm^2 in 1 s in response to an osmotic gradient of 1 mOsm per cc or 1 osmol per liter,
- C_i = the osmolarity of the water inside the epithelial cells,
- C_{film} = the osmolarity of the water at the open end (i.e., inside the film, along the vaginal lumen),
- D_s = the diffusion coefficient of the actively transported solute,
- $N(z)$ = the rate of active solute transport across the walls of the channel into its lumen at any height z, defined as milliosmols of solute transported in 1 s across 1 cm^2 of channel wall area (passive solute movement across the channel walls is assumed to be negligible),
- $C(z)$ = the osmolarity of the water in the channel at a height z,
- $v(z)$ = the linear velocity of water flow in the channel at height z, taken as positive in the direction $z = 0$ to $z = L$.

The assumptions made in this analysis and the details of the derivation of this transport mechanism can be found in Ref. 21. We have supplemented our bi-component, non-Newtonian, elastohydrodynamic flow model with the standing-gradient osmotic model in order to account for fluid that is being released into the film. Boundary conditions for the standing-gradient osmotic model can be given as

$$\begin{aligned} &\text{at } z = 0, \frac{dC}{dz} = \frac{d^2v}{dz^2} = 0, \\ &\text{at } z = 0, v = 0, \\ &\text{at } z = L, C = C_{film}, \frac{dv}{dz} = \frac{2P(C_{film} - C_i)}{r}. \end{aligned} \tag{9}$$

Note that the last boundary condition is defined in Ref. 21 as: at $z = L$, $C = C_i$, $dv/dz = 0$. Here, we assume that, at the open end, the osmolarity of the water moving inside the channels approaches the osmolarity of the water within the vaginal lumen, C_{film}.

An effective length of the channel, L, must be defined for stratified epithelium owing to its layer-over-layer structure. As the film is placed into the lumen, it distends the vaginal epithelium. To the best of our knowledge, there are no experimental data on the geometrical deformation of the epithelium (e.g., change in orientation of epithelial cells or alteration of the paracellular channels). Here, we assume that the epithelium thickness between the serosal side and the apical side depends exponentially on the compliance ratio of the serosal side and the apical side. Thus, we supplement our model with an additional compliance, to model the compression of the epithelium and thus the varying distance between the lumen and the serosal side. Then, the height profile of serosal side, $h_2(x, t)$,

$$h_2(x,t) = h(x,t) + L_1 \exp\left[-\frac{(h(x,t) - h_\infty)M_2}{HM_1}\right], \tag{10}$$

where M_1/M_2 characterizes the thickness of the epithelium.

We solve Eq. (8) separately from the governing film-water flow equation, Eq. (3). Equation (8) is solved with a shooting method owing to the nature of the boundary conditions. This gives us the velocity at the open end of the channel for a specified L and C_{film} value. Equation (8) is solved for a representative range of L, from 10 μm to 100 μm, and for a practical range of C_{film}, from 0.3 Osm (isotonic) to 2 Osm (hypertonic). Then, $v(z = L)$ as a function of L for $C_{film} = 0.3$, 0.6, 1, and 2 Osm, is plotted in Fig. 6. We set $r = 0.05$ μm, $C_i = 0.3$ Osm, $D = 10^{-6}$ cm^2/s, $N = 10^{-6}$ mOsm/cm^2/s for $0 < z < 10$ μm and at zero for $z > 10$ μm, and $P = 10^{-6}$ cm/Osm/s.[21] Here, for different values of L, we confine all solute transport to the bottom tenth of the channel. Clearly, further physiological characterization of the vaginal wall is required for a more accurate set of parameters and a more sophisticated theoretical treatment of the varying distance of LIS across the epithelium.

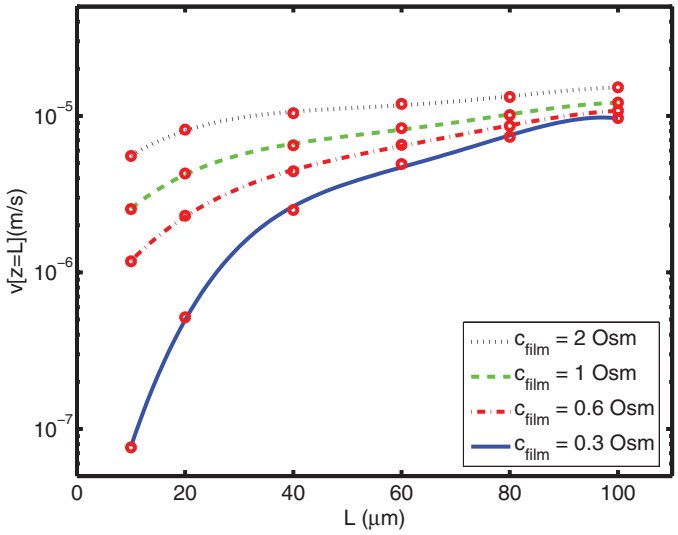

FIG. 6. Velocity (circles) at the open end ($z = L$) obtained by Eq. (8) for several L and C_{film} values.

The curve-fit of the results in Eq. (8) is found to be

$$\log v(z = L) = p_0 + p_1 L + p_2 L^2 + p_3 L^3 + p_4 L^4, \tag{11}$$

where the coefficients of the curve-fits are given in Table II.

Note that the water velocity in the channel is defined as, $q_{LIS} = v(z = L) = w \cdot q$. Here, w is the relevant factor or "porosity" of the epithelial layer. For vaginal epithelium, further experimental work is a prerequisite to determine the widths of the channels between the epithelial cells that can enable one to evaluate the porosity. Hence, due to the variability of the sizes of vaginal epithelial cells and its stratified structure, we shall make use of the porosity value of a relatively simpler structure, i.e., rabbit corneal epithelium (single layer squamous epithelium) $w \approx 100$.[16,22,23] Importantly, this value of the porosity brings the fluxes shown in Fig. 6 into the range of experimentally observed values.

Following the derivation of the wall fluid velocity, we now consider a simulation of the coating flow of the film ($M_1/M_2 = 0.1, C_{film} = 0.6$). Height profile of a prototype film is plotted as a function of time in Fig. 7(a). As can be seen from the figure, film begins to spread more due to varying rheology. The evolution of the volume fraction of film as a function of longitudinal position is plotted in Fig. 7(b). At $t = 0$, film is already swollen and dissolved. The initial volume-based swelling ratio, $vbsr$, is set to 4.0. To switch from swelling ratio to volume fraction of film, $vbsr = (1 - \phi)/\phi$ is used. As time passes, volume fraction of film decreases due to the incoming water flux.

Height profile of the bolus at 60 min and coating area as a function of time are plotted for a range of compliance ratios, $M_1/M_2 = 0.1$, 0.25, 1, and 100 in Fig. 8. Here, the water osmolarity at the open end, C_{film} is set to 0.6, to model a hypertonic film. As can be seen from the figure, the compliance ratio does not have a significant influence on the coating area.

TABLE II. The coefficients of the curve-fit for $C_{film} = 0.3$ (isotonic), 0.6, 1, and 2 Osm.

C_{gel}	p_4	p_3	p_2	p_1	p_0
0.3	-1.25×10^{-7}	3.39×10^{-5}	-3.42×10^{-3}	0.16	−8.42
0.6	-3.71×10^{-8}	1.00×10^{-5}	-1.01×10^{-3}	0.05	−6.36
1	-3.83×10^{-8}	1.01×10^{-5}	-9.62×10^{-4}	0.04	−5.95
2	-3.11×10^{-8}	8.32×10^{-6}	-7.91×10^{-4}	0.03	−5.52

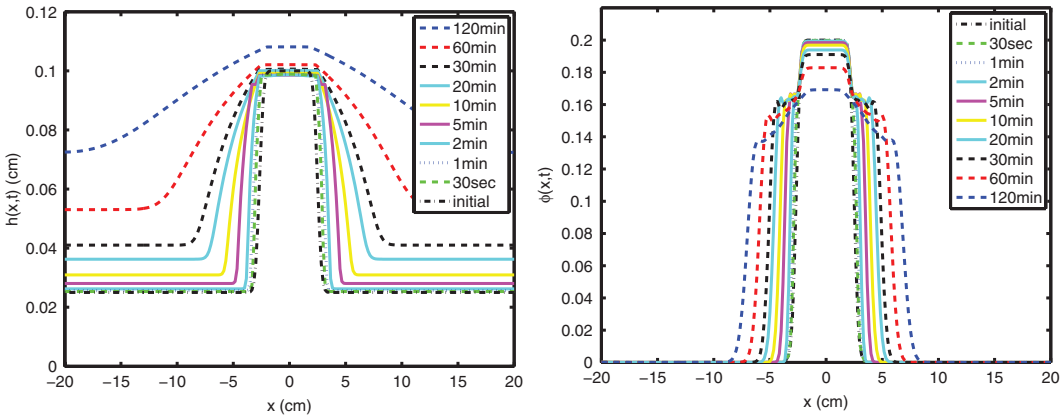

FIG. 7. (Left) Height profile of film and (right) volume fraction of film as a function of time ($M_1/M_2 = 0.1$, $C_{film} = 0.6$).

Next, we maintain the compliance ratio, M_1/M_2 at 0.1, and vary the water osmolarity at the open end, C_{film}. Height profiles of the bolus at 60 min and coating area as a function of time are plotted for $C_{film} = 0.3$ (isotonic), 0.6, 1, and 2 in Fig. 9. As can be seen from the figure, as the water osmolarity at the open end (or "thirstiness") of the film increases, boundary flux and coating area increase.

Of course, as more fluid is exuded from the vaginal wall, the dilution and hence also local osmolarity of the film can be expected to change. We did not couple the local dynamic osmolarity (related to ϕ) with the paracellular channel end condition C_{film} in the foregoing simulations, in view of the fairly significant assumptions that we have had to make regarding various physiological parameters. When the model can be improved with more relevant parameters, making the local dynamic osmolarity in the simulation respond to inhomogeneous boundary dilution is straightforward.

2. Drug absorption

We assume that drug absorption and elimination follow first order kinetics:[24]

$$\frac{dM_{pl}}{dt} = k_a F M_v - k_{el} M_{pl}. \tag{12}$$

The M_v and M_{pl} represent the amount of drug on the vaginal boundary and the volume absorbed as reflected in the plasma, respectively. M_v can be extracted from the solution of concentration distribution of drug molecules that is evaluated at each time step. F is the fraction of drug that enters

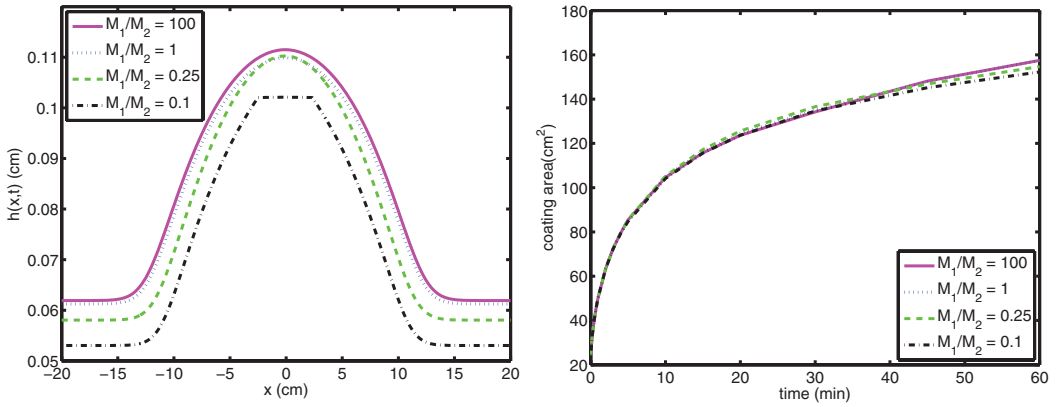

FIG. 8. (Left) Height profile of film at 60 min and (right) coating area of the film on the surface for $M_1/M_2 = 0.1$, 0.25, 1, and 100. ($C_{film} = 0.6$).

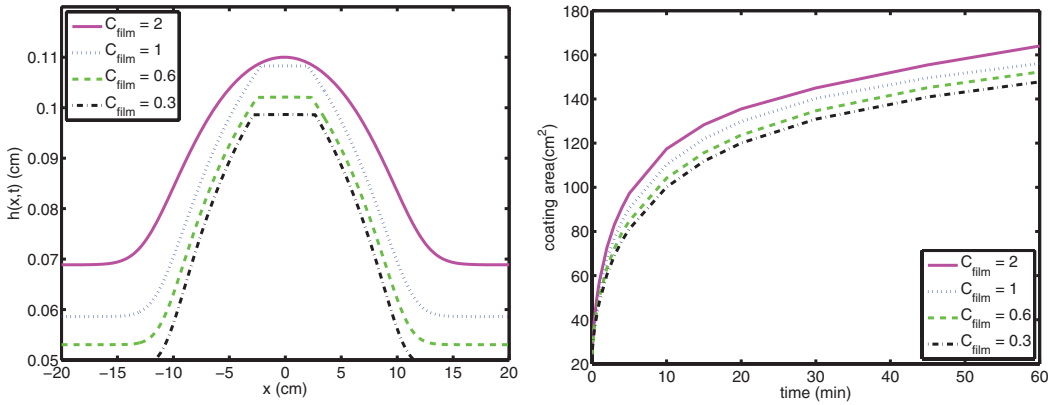

FIG. 9. (Left) Height profile of film at 60 min and (right) coating area of the film on the surface for $C_{film} = 0.3$, 0.6, 1, and 2. ($M_1/M_2 = 0.1$).

the circulation at serosal side; k_a and k_{el} are first-order rate constants of absorption and elimination from plasma, respectively. A contour plot of drug distribution in the reproductive tract is shown in Fig. 10 for time = 1, 10, 30, and 120 min. The initial condition for drug concentration is set as 0.1 mol/m^3 (molecular weight = 287.21 g/mol). The absorbed amount of Tenefovir at 2 h is plotted in Fig. 11 for a range of Fk_a ($F = 100$, $k_a = 0.005$, 0.01, 0.1 min^{-1} (Ref. 25)), and k_{el} (0.0001 to 0.01 min^{-1} (Ref. 25)). As can be seen from the figure, combined effect of Fk_a is significant on absorbed amount of Tenefovir, while the effect of k_{el} was limited.

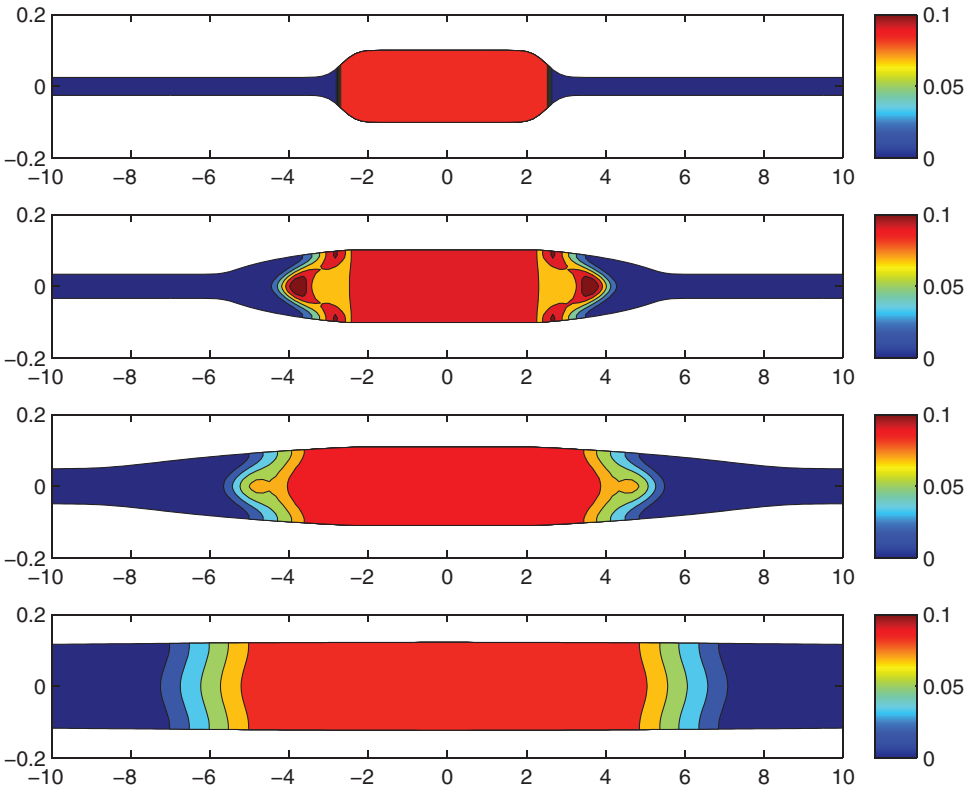

FIG. 10. Contour plot for drug distribution at time 1, 10, 30, and 120 min (initial concentration = 0.1 mol/m^3).

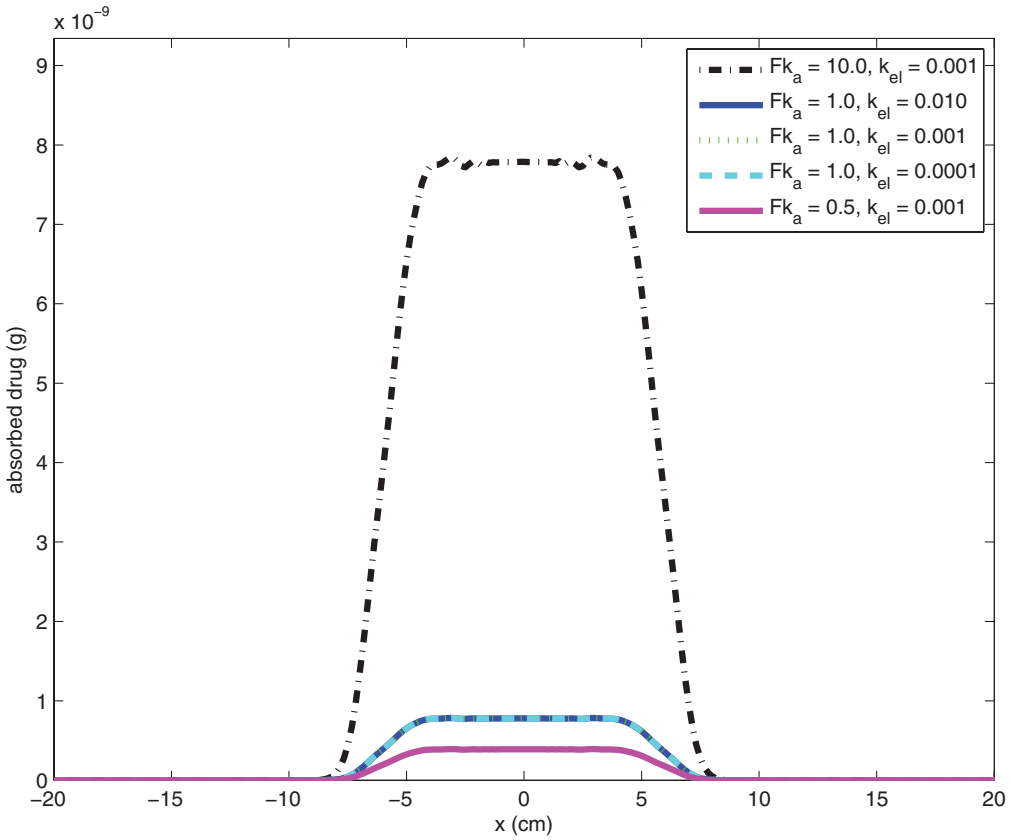

FIG. 11. Tenefovir absorption at 2 h for a range of Fk_a and k_{el}.

The paracellular routes between epithelial cells might also provide a convenient environment for drug absorption. For paracellular transport, first the physical size of Tenofovir molecule must be estimated and then compared with the intercellular spaces between vaginal epithelial cells. The physical size of the Tenofovir molecule is not reported in the literature. It is mainly composed of an adenine and a phosphonic acid. A simple length scale, l can be calculated by $l = (m/\rho/N_A)^{1/3}$. Here, N_A is Avagadros number and $N_A = 6.022 \times 10^{23}$ mol^{-1}. The molar masses, M, the densities, ρ, and the calculated lengths, l, of these individual structures are given in Table III. As can be seen from Table III, the total length is ~10 Å. The intercellular spaces between vaginal epithelial cells differ from layer to layer.[26] To the best of our knowledge, there is not any reported value for the lateral intercellular spaces between vaginal epithelial cells. However, they are reported as ~30 Å for corneal endothelial cells,[27] and ~240 Å for intestinal epithelial cells.[28] In this paper, we shall not further pursue paracellular transport of drug molecules. However, it can be concluded that Tenofovir molecules are likely physically smaller than the intercellular spaces at the vaginal epithelium, and paracellular transport of Tenofovir may take place, which most probably accompanies the reabsorption of vaginal fluid.

TABLE III. The molar masses, the densities and the lengths of phosphonic acid and adenine.

	M (g/mol)	ρ (g/cm^3)	Length (Å)
Phosphonic acid	82	1.651	4
Adenine	135.13	1.6	5.2

IV. CONCLUSIONS

There is a widespread agreement that more effective drug delivery vehicles with more alternatives, as well as better active ingredients, must be developed to raise the efficacy of anti-HIV microbicides. In this setting, here we studied topical films as an alternative to gels, which are widely studied in the literature.[4–7,29–31]

We first experimentally investigated the effects of dilution and swelling by ambient vaginal fluids on the rheological properties of the film formulations. The rheological parameters were obtained at equilibrium for plausible swelling ratios. The zero-shear viscosity, m_0, values were much higher than those of gels analyzed in our earlier works.[4–7,29] The Carreau constitutive model was fitted to the rheological data. Then, we integrated the rheological data into the mathematical model of the film spreading. The film formulations with a range of swelling ratio 3 to 5, i.e., estimated range in real applications, coated less area than that which was coated by homogeneously diluted gels we have studied before.

Next, we developed a model for transient swelling and spreading of a prototype film formulation designed for vaginal microbicide drug delivery. The model took into consideration further swelling of an initially dissolved film, and subsequent distribution of Tenofovir drug molecules throughout the vaginal lumen. The association between swelling of the film and its rheological properties was obtained experimentally, delineating the way constitutive parameters are modified by swelling and dilution.

Then, we explored a hypothetical time- and space-varying boundary flux mechanism. We modified the standing-gradient osmotic flow model[21] to take into consideration the osmotic gradients that may drive fluid through the epithelial tissue underlying a hypertonic film. This flow is thus due to active transportation of solute into the LIS, diffusion towards the mouth open to the vagina lumen, and hyperosmolarity of the film. We note that vaginal boundary flux can be defined in two different ways: flux per LIS and flux per unit area of the vaginal surface. To switch from one to another, a factor called porosity, w, is used[23] and the formula, $q_{LIS} = w \cdot q$, is employed. The simple structure of corneal endothelium allows one to calculate its geometry and thus the porosity with reasonable plausability.[16,23] However, vaginal epithelium is relatively complex. To the best knowledge of the authors, there is not sufficiently detailed information in the literature about the widths of the channels between the vaginal epithelial cells that can enable one to evaluate the porosity. Also accounting for the variability of the sizes of vaginal epithelial cells due to its stratified structure, we used the porosity value of a relatively simpler structure, i.e., rabbit corneal epithelium. The model outputs vaginal fluid fluxes at rates, $q_{LIS} \sim 10^{-7}$-10^{-5} or dividing q_{LIS} by porosity, $q \sim 10^{-9}$-10^{-7} −comparable to experimental data on such production. We accounted for the hypertonic property of these microbicide films by changing the boundary condition of the standing-gradient osmotic flow model at the open end of channels. Although we did not couple the evolving water concentration of the film, which is evaluated at each time step by the present model, with the osmolarity at the open end of channels, it is straightforward as long as the osmotic coefficient is known for the specific dissolved film employed. Here, instead we set constant values, from isotonic (0.3 Osm) to hypertonic (0.6, 1, and 2 Osm), for the osmolarity at the open end of channels.

We emphasize that there is a dearth of physiological information about the parameters for flows driven by osmotic forces across the vaginal epithelium. The parameters that characterize them are summarized in Sec. III of this paper. In the literature, they have been estimated for relatively simpler models, such as corneal epithelium. Clearly, such information for vaginal epithelium would not only improve the biophysical accuracy of the modeling here, but can be of broad biomedical relevance to women's health. In addition, for osmotic boundary flux, a simple model is employed in the present paper to evaluate varying distance between the apical and the serosal side of vaginal epithelium. This provided the effective lengths of the channels along the vaginal lumen. Further experimental works that investigate the effects of any pressure force on the effective lengths of lateral intracellular spaces is a prerequisite for more sophisticated understanding of transport across the vaginal epithelium, and in general, any stratified epithelium.

For the absorption of drug molecules, we proposed a straightforward transcellular boundary condition integrated with a first-order kinetic equation. Results showed that the first-order rate

constant of absorption had a significant effect on absorbed amount of Tenefovir, while the effect of the elimination coefficient was limited. Also, we argued the plausibility of paracellular drug transport. We pointed out the likelihood that the size of Tenofovir molecule is small enough to allow it to move within the intercellular spaces between the vaginal epithelial cells. Clearly, further experimental work is a prerequisite to model transcellular and paracellular transport of Tenofovir.

The theory developed here for a swelling microbicide film and its impact on the course of the films vaginal deployment will be useful to the microbicide community. The theory developed here improves our understanding of the biophysics of microbicide film flows *in vivo*, which can lead to improved understanding of drug delivery by those films. In addition, the theory here may find application in other elastohydrodynamic problems of interest.

ACKNOWLEDGMENTS

D.F.K. acknowledges support from NIH grants (Grant Nos. U19 AI077289 and RO1 HD 072702). S.T. acknowledges support from The Scientific and Technological Research Council of Turkey (Tubitak).

[1] S. L. Kieweg, A. R. Geonnotti, and D. F. Katz, "Gravity-induced coating flows of vaginal gel formulations: *In vitro* experimental analysis," J. Pharm. Sci. **93**, 2941 (2004).
[2] S. L. Kieweg and D. F. Katz, "Squeezing flows of vaginal gel formulations relevant to microbicide drug delivery," J. Biomech. Eng. **128**, 540 (2006).
[3] S. L. Kieweg and D. F. Katz, "Interpreting properties of microbicide drug delivery gels: Analyzing deployment due to squeezing," J. Pharm. Sci. **96**, 835 (2007).
[4] A. J. Szeri, S. C. Park, S. Verguet, A. Weiss, and D. F. Katz, "A model of transluminal flow of an anti-HIV microbicide vehicle: Combined elasticsqueezing and gravitational sliding," Phys. Fluids **20**, 083101 (2008).
[5] S. Tasoglu, S. C. Park, J. J. Peters, D. F. Katz, and A. J. Szeri, "The consequences of yield stress on deployment of a non-Newtonian anti-HIV microbicide gel," J. Non-Newtonian Fluid Mech. **166**(19–20) 1116–22 (2011).
[6] S. Tasoglu, J. J. Peters, S. C. Park, S. Verguet, D. F. Katz, and A. J. Szeri, "The effects of inhomogeneous boundary dilution on the coating flow of an anti-HIV microbicide vehicle," Phys. Fluids. **23**, 093101 (2011).
[7] S. Tasoglu, D. F. Katz, and A. J. Szeri, "Transient spreading and swelling behavior of a gel deploying an anti-HIV topical microbicide," J. Non-Newtonian Fluid Mechanics **187–188**, 36–42 (2011).
[8] C. Coggins, C. J. Elias, R. Atisook, M. T. Bassett, V. Ettiegnene-Traore, P. D. Ghys, L. Jenkins-Woelk, E. Thongkrajai, and N. L. VanDevanter, "Women's preferences regarding the formulation of over-the-counter vaginal spermicides," AIDS **12**, 1389–91 (1998).
[9] S. Garg, K. Vermani, A. Garg, R. A. Anderson, W. B. Rencher, and L. J. D. Zaneveld, "Development and characterization of bioadhesive vaginal films of sodium polystyrene sulfonate (PSS), a novel contraceptive antimicrobial agent," Pharm. Res. **22**, 584–595 (2005).
[10] S. Roy, *Barrier Contraceptives: Current Status and Future Prospects* (Wiley, New York, 1994).
[11] D. J. Coyle, "Forward roll coating with deformable rolls: A simple one-dimensional elastohydrodynamic model," Chem. Eng. Sci. **43**, 2673 (1988).
[12] J. M. Skotheim and L. Mahadevan, "Soft lubrication," Phys. Rev. Lett. **92**, 245509 (2004).
[13] A. Steinberger, C. Cottin-Bizonne, P. Kleimann, and E. Charlaix, "Nanoscale flow on bubble mattress: Effect of surface elasticity," Phys. Rev. Lett. **100**, 134501 (2008).
[14] J. Chakraborty and S. Chakraborty, "Combined influence of streaming potential and substrate compliance on load capacity of a planar slider bearing," Phys. Fluids **23**, 082004 (2011).
[15] D. H. Owen and D. F. Katz, "A vaginal fluid stimulant," Contraception **59**, 91–95 (1999).
[16] W. H. Masters and V. E. Johnson, *Human Sexual Response* (Little, Brown, Boston 1966).
[17] Q. A. Abdool Karim *et al*. "Effectiveness and safety of Tenofovir del, an antiretroviral microbicide, for the prevention of HIV infection in women," Science **329**, 1168–1174 (2010).
[18] A. R. Geonnotti, M. J. Furlow, T. Wu, M. G. DeSoto, M. H. Henderson, P. F. Kiser, and D. F. Katz, "Measuring macrodiffusion coefficients in microbicide hydrogels via postphotoactivation scanning," Biomacromolecules **9**, 748–51 (2008).
[19] K. Podual, F. Doyle III, and N. A. Peppas, "Modeling of water transport in and release from glucose-sensitive swelling-controlled release systems based on poly (diethylaminoethyl methacrylate-g-ethylene glycol)," Ind. Eng. Chem. Res. **43**, 7500 (2004).
[20] B. E. Lai, Y. Q. Xie, M. Lavine, A. J. Szeri, D. H. Owen, and D. F. Katz, "Dilution of microbicide gels with vaginal fluid and semen simulants: Effects on rheology and coating flow," J. Pharm. Sci. **97**, 1030 (2008).
[21] J. M. Diamond and W. H. Bossert, "Standing-gradient osmotic flow: A mechanism for coupling of water and solute transport in epithelia," J. Gen. Physiol. **50**(8), 2061–83 (1967).
[22] L. Langbein, C. Grund, C. Kuhn, S. Praetzel, J. Kartenbeck, J. M. Brandner, I. Moll, and W. W. Franke, "Tight junctions and compositionally related junctional structures in mammalian stratified epithelia and cell cultures derived therefrom," European J. Cell Biol. **81**(8), 419–35 (2002).

[23] J. Fischbarg and F. P. J. Diecke, "A mathematical model of electrolyte and fluid transport across corneal endothelium," J. Membr. Biol. **203**, 41–56 (2005).
[24] M. Rowland and T. N. Tozer, *Clinical Pharmacokinetics: Concepts and Applications*, 3rd ed. (Williams and Wilkins, Media, PA, 1995).
[25] H. H. Usansky and P. J. Sinko, "Estimating human drug oral absorption kinetics from caco-2 permeability using an absorption-disposition model: Model development and evaluation and derivation of analytical solutions for ka and Fa," J. Pharmacol. Exp. Ther. **314**, 391–399 (2005).
[26] M. Hackemann, C. Grubb, and K. R. Hill, "The ultrastructure of normal squamous epithelium of the human cervix uteri," J. Ultrastruct. Res. **22**, 443–457 (1968).
[27] A. Rubashkin, P. Iserovich, J. A. Hernandez, and J. Fischbarg, "Epithelial fluid transport: Protruding macromolecules and space charges can bring about electro-osmotic coupling at the tight junctions," J. Membr. Biol. **208**, 251–263 (2005).
[28] M. G. Farquhar and G. E. Palade, "Junctional complexes in various epithelia," J. Cell. Biol. **17**, 375–412 (1963).
[29] S. Tasoglu, "Transport phenomena and pharmacokinetics of anti-HIV microbicide drug delivery," Ph.D. dissertation, University of California, Berkeley, 2011.
[30] S. Tasoglu, A. J. Szeri, and D. F. Katz, "Transport processes in vaginal films that release anti-HIV microbicide molecules," Biophys. J. **100**(3), 489a (2011).
[31] A. J. Szeri, S. C. Park, S. Tasoglu, S. Verguet, A. Gorham, Y. Gao, and D. F. Katz, "Epithelial coating mechanisms by semi-solid materials: Application to microbicide gels," Biophys. J. **98**(3), 604a–604a (2010).